The Astrophysical Journal, 896:152 (11pp), 2020 June 20 https://doi.org/10.3847/1538-4357/ab910b
© 2020. The American Astronomical Society. All rights reserved.

Effect of Binarity in Star Cluster Dynamical Mass Determination

Sara Rastello[1,2,3], Giovanni Carraro[2], and Roberto Capuzzo-Dolcetta[1]
[1] Dipartmento di Fisica, Sapienza, Universitá di Roma, P.le A. Moro 5, I-00185 Roma, Italy
[2] Dipartimento di Fisica e Astronomia, Universitá di Padova, Vicolo Osservatorio 3, I-35122 Padova, Italy; giovanni.carraro@unipd.it
[3] INFN-Padova, Via Marzolo 8, I-35131 Padova, Italy
Received 2020 January 31; revised 2020 May 2; accepted 2020 May 5; published 2020 June 23

Abstract

In this paper we explore the effects that the presence of a fraction of binary stars has in the determination of a star cluster mass via the virial theorem. To reach this aim in an accurate and consistent way, we run a set of simulations using the direct summation, high precision, code NBODY7. By means of this suite of simulations we are able to quantify the overestimate of open-star-cluster-like models' dynamical masses when making a straight application of the virial theorem using available position and radial velocity measurements. The mass inflation caused by the binary "heating" contribution to the measured velocity dispersion depends, of course, on the initial binary fraction, f_{b0} and its following dynamical evolution. For an f_b (evolved up to 1.5 Gyr) in the range 8%–42% the overestimate of the mass done using experimentally sounding estimates for the velocity dispersion can be up to a factor of 45. We provide a useful fitting formula to correct the dynamical mass determination for the presence of binaries, and underline how neglecting the role of binaries in stellar systems might lead to erroneous conclusions about their total mass budget. If this trend remains valid for larger systems like dwarf spheroidal galaxies, which are still far out of reach for high-precision dynamical simulations taking their binaries into account, it would imply an incorrect overestimation of their dark matter content, as inferred by means of available velocity dispersion measurements.

Unified Astronomy Thesaurus concepts: Binary stars (154); Star clusters (1567); N-body simulations (1083)

1. Introduction

Binary stars play a very important role in the dynamics of stellar systems, from small open-star clusters (Hut et al. 1992) to dwarf spheroidal galaxies (Spencer et al. 2017). There are both observational and numerical indications that binaries observed in stellar systems (from loose open clusters to very dense globular clusters) cannot be entirely explained by dynamical formation processes, such as three-body dynamics or two-body tidal capture (Aarseth & Lecar 1975), but should be, rather, primordial (Hut et al. 1992; Portegies Zwart et al. 2001; Binney & Tremaine 2008; Kouwenhoven & de Grijs 2008). This fraction of tight primordial binaries may affect dynamical mass estimates most.

The dynamical evolution of a star cluster depends strongly on its binary population: even a small initial binary fraction can play a fundamental role in governing cluster dynamics and the whole cluster stellar evolution (see, for instance, Goodman & Hut 1989; McMillan et al. 1990, 1991; Hut et al. 1992; Mathieu 1994; McMillan & Hut 1994; Portegies Zwart et al. 2001; Goodwin & Kroupa 2005; Kouwenhoven et al. 2007; Kouwenhoven & de Grijs 2008, and references therein). However, the influence of binaries on properties like the bulk motion and velocity dispersion of stellar systems has not yet been fully characterized and understood. From an observational point of view it is a challenging task to catch the entire binary population of a stellar system, because binaries can have very different periods (Geller & Mathieu 2012), and this induces a clear bias in the determination of the binary fraction in a cluster if only one or a few epochs are observed, as is customary. Usually, binaries can be detected in one of the following ways: by spectroscopy (from radial velocity variations), or photometry (from the abnormal location on Hertzsprung–Russell diagram). Other types of binaries are the so-called "visual" binaries (stars too close on the sky to be explained by chance projection; Goodwin 2010) and the astrometric binaries (visual binaries that we see orbiting). Clearly, all of these methods are biased; the first method is biased to close similar-mass companions while the second and the third methods are biased toward similar-luminosity or -mass (low-mass) companions (Goodwin & Kroupa 2005; Goodwin 2010).

In globular clusters, the fraction of binaries is regulated by two competing effects: the formation of bound systems due to dynamical segregation, and their destruction due to strong dynamical interactions in the cluster cores (Ji & Bregman 2013, 2015a, 2015b).

In looser systems, like open clusters or dwarf galaxies, strong dynamical interactions are rare, and primordial binaries may survive longer (Portegies Zwart et al. 2001). The fraction of primordial binaries in open clusters is estimated to range between 30% and 60% (Portegies Zwart et al. 2001; Sana et al. 2008, 2009, 2011, 2013) approaching 100% in some particular cases (Fan et al. 1996; de la Fuente Marcos & de la Fuente Marcos 2008; Sana et al. 2008).

In dwarf galaxies, in particular, the presence of binary stars has been considered as a potential explanation for the difference in velocity dispersion with respect to globular clusters of comparable mass. Actually, the velocity dispersion in dwarf galaxies is, typically, larger, and also the mass to light ratio, which would imply a very large content of dark matter (Spencer et al. 2017).

The possible link between dark matter content and binary fraction is particularly intriguing. Globular clusters are dark matter free, and host small fractions of binaries. On the other side, dwarf spheroidal galaxies (Spencer et al. 2017) seem to be dark matter dominated and, at the same time, they host many binaries. The bridge between dark matter content and binary content could be the velocity dispersion, via the virial theorem. Previous studies showed that when binary stars are properly taken into account the velocity dispersion estimation and, in

turn, the evaluation of the virial mass of dwarf galaxies tend to decrease (Spencer et al. 2017, 2018).

Therefore, the knowledge of the binary content of a stellar system allows us to clear the bias they induce: the better they are taken into account, the smaller the velocity dispersion results are (Kouwenhoven & de Grijs 2008; Spencer et al. 2017). This issue is particularly crucial for low density systems, like Bootes I (Muñoz et al. 2006; Koposov et al. 2011), or Segue 1 (Geha et al. 2009; Martinez et al. 2011; Simon et al. 2011).

Direct measurements of the 1D velocity dispersion ($\sigma_{\rm los}$) of a star cluster can be done in three different ways: (i) estimating the width of spectral lines from observations spanning a significant part of the cluster (Moll et al. 2009); (ii) measuring the radial velocities of individual stars (Apai et al. 2007), and (iii) proper motions (Chen et al. 2007; Tofflemire et al. 2014), possible only for nearby clusters. Due to the nature of the observations, the velocity dispersion obtained using techniques (i) and (ii) might be significantly affected by the presence of binaries (Kouwenhoven & de Grijs 2008), while proper motion measurements do not lead to a mass overestimation, even when the binary fraction is high. For instance, single-epoch velocity dispersion is larger than multiepoch velocity dispersion, and the wider the time coverage, the smaller the resulting velocity dispersion. This means that binary stars can "inflate" the velocity dispersion of stellar systems. In fact, in a cluster consisting only of single stars, the velocity dispersion strictly correlates with the motion of each "particle" in the cluster potential. On the other hand, in a cluster populated also by binary stars we cannot easily pick the motion of the binary center of mass from that of the individual binary components, which gives two additional degrees of freedom (like roto-vibrations in a diatomic molecule), the rotational one being dominant. This may induce, thus, an overestimation of the dynamical cluster mass (Fleck et al. 2006; Apai et al. 2007; Gieles et al. 2010) as computed using the virial theorem.

Given all the above, we note that, interestingly, the mean stellar density and binary fraction of dwarf spheroidal galaxies is comparable to that of open clusters in the Milky Way disk (McConnachie 2012; Kharchenko et al. 2013; Spencer et al. 2018). It is therefore tempting to start systematically testing the binary effect on open clusters first, given the obvious numerical advantage, to look for similarities and/or differences with observations.

Open clusters are in fact small enough to allow us to perform multiple simulations of their dynamics at a level sufficient to give good statistical coverage of their properties, yet they are large enough and old enough that both stellar evolution and stellar dynamics have had time to play significant roles in determining their present structure. (Portegies Zwart et al. 2001).

Moreover, open clusters contain fractions of binaries larger than the globular cluster (de la Fuente Marcos & de la Fuente Marcos 2008; Carraro et al. 2017), and are widely accepted to be devoid of dark matter halos. The small number of stars belonging to open clusters allows a tight comparison with numerical models.

Generally, high precision dynamical models studied so far, exclude binaries for simple practical reasons (Mikkola & Aarseth 1998; Portegies Zwart et al. 2001; Trenti et al. 2007): (i) binaries slow down calculations dramatically and induce huge numerical errors; (ii) their internal evolution is much more complicated than the evolution of single stars; (iii) a good treatment of binaries would require accurate dynamical regularization tools.

However, from a theoretical/numerical side, given the relatively small number of open clusters' member stars it is easy to explore the role of binaries in such systems.

In this paper we address the role of binaries in open cluster-like stellar systems in influencing the cluster velocity dispersion and thus the determination of the cluster "dynamical" mass. Our work is based on high precision, direct summation, *N*-body simulations. With the aim to span a wide range of initial conditions, we model open clusters at varying the initial fraction of primordial binaries and the cluster initial virial state (by means of varying the initial virial ratio $Q = 2T/|\Omega|$, where T and Ω are the total kinetic and potential energy, respectively; $Q = 1$ corresponds to virial equilibrium). Although this is the most straightforward definition of a virial ratio, coming directly from the expression of the second time derivative of the polar moment of inertia of a system of N gravitating objects, we note that some papers refer to the virial ratio as the $Q = T/|\Omega|$ ratio, that gives $1/2$ for a virialized system. To estimate the velocity dispersion of the cluster, and hence the system kinetic energy, we use three different methods, accounting in different ways for the presence of binary stars.

The paper is organized as follows: in Section 2 we describe the models and the numerical methods we used; in Section 3 we present and discuss our results. Summary and conclusions are drawn in Section 4.

2. Method and Models

2.1. N-body Models

In order to study the effect of binaries on the estimation of the dynamical mass of open clusters we made use of high precision direct *N*-body simulations performed with the code NBODY7 developed by Nitadori & Aarseth (2012). NBODY7 is a direct summation *N*-body code that integrates in a reliable way the motion of stars in not too abundant stellar systems and that implements sophisticated and efficient recipes to deal with strong gravitational encounters, taking also into account stellar evolution. The high precision treatment of binary stars is allowed in NBODY7 thanks to the KS regularization tool (Kustaanheimo & Stiefel 1965) and the Algorithmic Regularization Chain (Mikkola & Tanikawa 1999).

We defined six simulation groups (A, B, C, D, E, and F) representing various open clusters, varying the population of primordial binaries and the cluster virial state. All the clusters initially contain $N_0 = 1000$ stars. In all cases, the radial distribution was set according to a Plummer density profile (Plummer 1911). The initial total mass of each cluster is, in dependence on the random seed for the sampling, in the interval 600–700 $M_\odot$. The cluster core radius is $r_c = 1$ pc, and for each system we adopt solar metallicity ($Z_\odot$). We assume a Kroupa (2001) initial mass function with masses in the range $0.01\ M_\odot \leqslant m \leqslant 100\ M_\odot$. The clusters are supposed to be isolated and considered as proxies of open clusters of the Milky Way.

For each model (A, B, C, D, E, and F) we vary the fraction of primordial binaries, f_{b0}, and the initial virial ratio, Q_0 (see Table 1).

Table 1
Summary of the Initial Conditions Adopted in Our Models

Model	f_{b0} (%)	Q_0
A	5	1
B	15	1
C	30	1
D	5	0.5
E	15	0.5
F	30	0.5

Note. The columns from left to right represent (1) the label of the model, (2) the percentage fraction of primordial binaries (f_{b0}), and (3) the initial virial ratio (Q_0) of the clusters.

The first three groups of simulations (A, B, and C) represent clusters in an initial virial equilibrium ($Q_0 = 1$) while the other groups (D, E, and F) refer to subvirial star clusters, assuming $Q_0 = 1/2$.

We consider for each cluster model a primordial population of binaries in a fraction that varies in the 5%–30% range (Table 1). The initial fraction of binaries, f_{b0} is defined as the ratio of the initial number of pairs of stars, N_{b0}, to the initial total number of cluster stars, N_0, so that $f_{b0} = N_{b0}/N_0$, and $N_0 = N_{s0} + 2N_{b0}$ is the total number of stars, provided N_s as the number of single stars in the system.

The mass ratio distribution of the primordial binary population is modeled according to the law $f(m_A/m_B) \propto (m_A/m_B)^{+0.4}$ (where $m_A \geqslant m_B$ are the masses of the two stars in the binary; Kouwenhoven et al. 2008), while periods are distributed according a logarithmic distribution (Kroupa 1995) and, for eccentricities (e), we assumed a "thermal" distribution $g(e) = 2e$ (Jeans 1919). For each model, we run 10 N-body simulations. Each simulation is a different realization of each cluster model for which we change the random "seed" when creating the initial conditions.

In particular, the initial conditions drawn this way are obtained by updating the procedure followed in Arca-Sedda et al. (2015). We evolved all the models up to ~1.5 Gyr. All the simulations were performed with the multi-GPU workstation ASTROC16A hosted at Sapienza, University of Rome.

2.2. Strategy

It is intuitive that binary stars play a relevant role when estimating the mass of a star cluster by means of virial considerations. This is because their presence can significantly affect the "observed" velocity dispersion, giving an extra contribution over the pure kinetic (translational) one that would provide the correct evaluation of kinetic energy at the numerator of the virial ratio Q. Of course, any overestimate of the kinetic energy, at a given Q value, leads to a corresponding overestimate of the mass of the system.

From an observational point of view, it is really challenging to disentangle the binary population, especially when binaries have long periods and small amplitudes, although long period binaries are the ones that less affect the velocity dispersion measurements because of their lower velocities around the pair barycenter. Typically, multiepoch and high precision radial velocity measurements are required. So, to evaluate the binary role it is much more feasible to use a "direct" and controlled approach, which means to build up a set of N-body realizations of a cluster whose binary content is predefined to get numerical outputs that allow one to check how the velocity dispersion evaluations can be biased. Therefore, we estimated the cluster 3D velocity dispersion in all of our models in Table 1 by means of four different methods, described as follows:

1. Method 1: the total velocity dispersion (hereafter, denoted with $\sigma_{\rm tot}$) is estimated accounting for all the stars of the cluster as if "they were all single stars," i.e., independently of possible binarity. In practice, given N velocity vectors, $\boldsymbol{v}_i$ ($i = 1,2, \ldots, N$), we scaled them to the proper rest frame to evaluate the total velocity dispersion
$$\sigma_{\rm tot} = \sqrt{\frac{1}{N}\sum_{i=1}^{N} v_i^2}, \quad (1)$$
where v_i is the absolute value of $\boldsymbol{v}_i$.
2. Method 2: here we make a distinction between the N_s single stars and the N_b binaries, in that, in the velocity dispersion calculation, we consider for every jth ($j = 1,2, \ldots, N_b$) binary composed by the two masses $m_{A,j}$ and $m_{B,j}$, only its center of mass velocity,
$$\boldsymbol{v}_{{\rm cm},j} = \frac{m_{A,j}\boldsymbol{v}_{A,j} + m_{B,j}\boldsymbol{v}_{B,j}}{M_j}, \quad (2)$$
where $M_j = m_{A,j} + m_{B,j}$ is the binary mass, to evaluate the cluster velocity dispersion as
$$\sigma_{\rm cm} = \sqrt{\frac{1}{N_s + N_b}\left(\sum_{i=1}^{N_s} v_i^2 + \sum_{j=1}^{N_b} v_{{\rm cm},j}^2\right)}. \quad (3)$$
3. Method 3: here we keep a distinction between single and binary stars but, in this case, for every binary we consider a luminosity averaged velocity
$$\boldsymbol{v}_{{\rm lum},j} = \frac{L_{A,j}\boldsymbol{v}_{A,j} + L_{B,j}\boldsymbol{v}_{B,j}}{L_j},$$
where $L_j = L_{A,j} + L_{B,j}$ is the binary total bolometric luminosity, so to have a dispersion, $\sigma_{\rm lum}$, defined as
$$\sigma_{\rm lum} = \sqrt{\frac{1}{N_s + N_b}\left(\sum_{i=1}^{N_s} v_i^2 + \sum_{j=1}^{N_b} v_{{\rm lum},j}^2\right)}. \quad (4)$$
4. Method 4: to have another term of comparison with observations, we also derived the velocity dispersion over the set of single stars only, thus excluding binary systems. The velocity dispersion, referred to as $\sigma_{\rm sing}$, is so
$$\sigma_{\rm sing} = \sqrt{\frac{1}{N_s}\sum_{i=1}^{N_s} v_i^2}. \quad (5)$$

Method 1 is the simplest possible estimate of the velocity dispersion, but it provides a value of the kinetic energy content that exceeds the actual (3 degrees of freedom per particle), contrasting the global potential, because, in a quantity dependent on the binary fraction, it accounts also for the binary inner degrees of freedom, which should not be considered in a virial mass determination. Actually, cluster observations suffer from the following issues: (i) for many reasons, we are able to identify only a fraction of cluster stars, usually the most luminous stars; (ii) binaries are difficult to detect and to distinguish with respect to single stars. This is

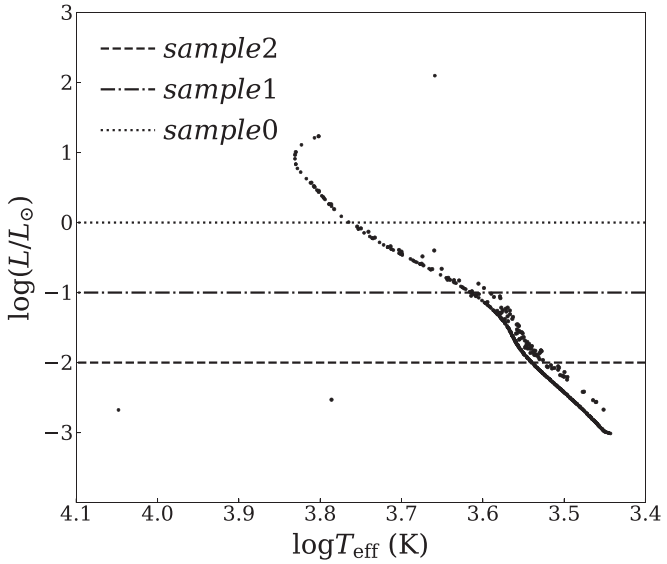

Figure 1. Example of the HR diagram for a simulation of model B at 1.5 Gyr. The three lines refer to the different luminosity cuts: dashed line for sample2, dotted–dashed line for sample1, and dotted line for sample0, respectively. The spread in the main sequence track is due to the binaries.

particularly true when dealing with binaries composed of two stars of significantly different luminosity. In this case it is really hard to derive the individual velocity components of the two binary stars with high precision and to pick the center of mass velocity. Thus the kinematic study requires a lot of radial velocity measurement data, spanning a wide range of time. Consequently, Method 3 is the closest to what happens when dealing with observations.

As said in Section 2.1, the evolution of our open-cluster models is followed up to ∼1.5 Gyr, the time at which we estimate the velocity dispersion according to the methods described above. In order to improve statistical significance we make averages over a time range ±50 Myr around 1.5 Gyr.

To give a reliable comparison with observations, we extract three different samples of stars from each model cluster based on their luminosity. We consider the (log $T_{\rm eff}$, log L) HR diagram as shown in Figure 1 and select three luminosity biased samples of stars according to the following thresholds (named according to the luminosity cut): (1) $\log(L/L_{\odot}) \geqslant -2$, hereafter addressed as sample2; (2) $\log(L/L_{\odot}) \geqslant -1$, hereafter addressed as sample1; and (3) $\log(L/L_{\odot}) \geqslant 0$, hereafter addressed as sample0.

Thus, for each model we estimate the velocity dispersion for each selected sample of luminosity. The error of the velocity dispersion is evaluated according to the standard deviation measures.

3. Results and Discussion

3.1. Cluster Dynamical Evolution

Many physical processes influence cluster evolution, among which the most important are stellar evolution, the Galactic tidal field, and the fraction of binary and multiple stars. The abundant mass loss from individual stars during their early evolution is of greatest importance and, carrying away much of the cluster binding energy, it may result in the disruption of the entire cluster (Portegies Zwart et al. 2001). If the cluster survives this early phase, stellar evolutionary timescales become longer than the timescales for dynamical evolution, hence two-body relaxation and tidal effects become dominant. Moreover, the presence of a population of primordial binaries is crucial to both stellar and dynamical evolution of a cluster (Hut et al. 1992). Actually, the mass transfer between binary components allows new stellar evolutionary states to arise and, in addition, the presence of binaries may enhance the rate and type of stellar collisions, making possible the temporary capture of single stars and other binaries in three-body encounters (Heggie 1975; Portegies Zwart & Yungelson 1998). In addition to the mass loss due to stellar wind, clusters also lose mass in the form of escaping stars. The fraction of escapers is enhanced if clusters are considered embedded in the external tidal field of the host galaxy (the escaper rate is estimated to be of the order of about 10% per relaxation time; Spitzer 1987). The external tidal field induces truncation of the cluster sizes and lowers the escape speed, significantly enhancing the mass-loss rate (Vesperini 2010). This makes the cluster dissolution time significantly shorter than in the isolated case. We stress here that in our models the clusters are all isolated systems. Although this assumption is surely questionable for real open clusters, which are embedded in an external potential and subjected to galactic differential rotation, it constitutes a needed initial step in this type of investigation. Isolated systems undergo mass loss through escapers as due to the combined effects of close and distant encounters (Heggie & Hut 2003).

Table 2
Some Parameters of the Model Clusters at $t = 1.5$ Gyr

Model	$\langle N \rangle$	$\langle M_{\rm cl} \rangle$ ($M_{\odot}$)	$\langle f_b \rangle$ (%)
A	730	290.20	5.6
B	723	279.40	17.1
C	706	275.60	35.1
D	637	251.87	6.3
E	614	240.98	18.9
F	601	240.19	37.9

Note. From left to right the various columns give (1) the model identification label (see Table 1); (2) the averaged number of bound stars ($\langle N \rangle$); (3) the mean cluster mass ($\langle M_{\rm cl} \rangle$; and (4) the mean percentage of binaries bound to the cluster ($\langle f_b \rangle = \langle N_b/N \rangle$). The reported values are averaged over all the simulations performed in each set.

A summary of the configuration of the clusters is given in Table 2, where we report the clusters' properties after 1.5 Gyr from the beginning of the simulations. The ±50 Myr indicates that the results are averaged over a time of 100 Myr around 1.5 Gyr.

We notice that in models corresponding to an initial virial equilibrium (A, B, and C) the number of retained stars (and thus the total bound mass $\langle M_{\rm cl} \rangle$) is larger (∼70%) with respect to models on a initial subvirial state (D, E, and F) after 1.5 Gyr. Additionally, initially virialized models show also a somewhat larger fraction of retained binaries: 5%, 17%, and 35%, which corresponds to ∼41, ∼123, and ∼250 binaries for models A, B, and C, respectively. In subvirial models, the effect of encounters is enhanced and leads to destruction of a large number of binaries, which are, after 1.5 Gyr, respectively, ∼40, ∼117, and ∼226 for model D, E, and F. The opposite trend in the fraction column of Table 2 is due to the fact that in the subvirial models the enhanced ejection of single stars covers the enhanced binary disruption.

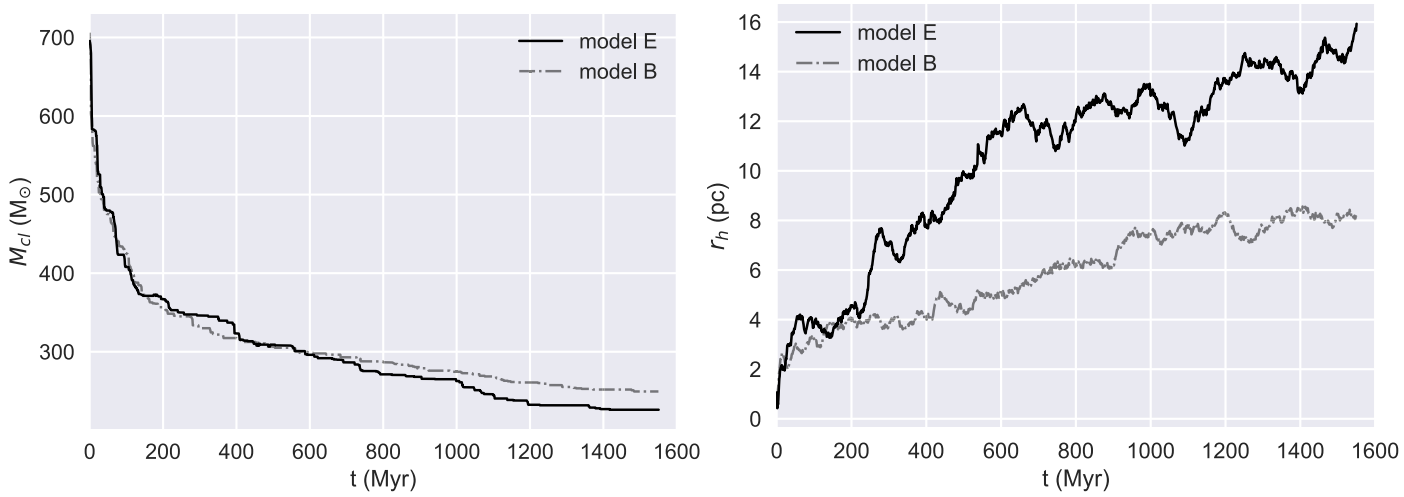

Figure 2. Evolution of the mass ($M_{\rm cl}$, left panel) and of the half-mass radius (r_h, right panel) for two of the simulations in the sets of models B (initial virial equilibrium) and E (subvirial).

A similar result is discussed in Sana et al. (2013). Note that initially we set $N_{b0} = 50$ for models A and D, $N_{b0} = 150$ for models B and E, and $N_{b0} = 300$ for models C and F.

Actually, primordial binaries may be disrupted or may exchange components with other stars, and, in addition, because of the gravitational interactions within the stellar systems, new binaries may form (Hut et al. 1992). However, in open-cluster-like systems strong gravitational encounters are rare and the disruption of binary systems is generally less pronounced (apart from wide binaries, which are likely to become unbound) with respect to globular clusters (Terlevich 1987). Moreover, binaries are generally heavier than single stars and tend to segregate toward the central region of the hosting star cluster, where the escape velocity is higher and, so, the probability to escape from the clusters is lower.

In Figure 2 we show the time evolution of the cluster mass ($M_{\rm cl}$) and of the half-mass radius (r_h) for two simulations of models B and E. We notice, in both cases, a quick mass loss from the systems (few hundreds of megayears) followed by a secular trend. Model E (initially subvirial) loses more mass than model B. Both systems globally (right panel) expand, but after ∼200 Myr, we notice that the half-mass radius of the initially subvirial model shows a larger expansion. This is a consequence of the initial violent collapse of model E whose following relaxation determines its further, secular, increased expansion and mass loss with respect to the virial case (model B; see also Terlevich 1987; Binney & Tremaine 2008).

3.2. Cluster Velocity Dispersion

As discussed in Section 2.2 (see Figure 1) we have extracted three samples of cluster stars from each model basing on different luminosity cutoff. We estimate the velocity dispersion for each sample by means of the four methods described in Section 2.2. Figure 3 shows the averaged cluster velocity dispersion at 1.5 Gyr as a function of the binary fraction for sample2, sample1, and sample0. The values of the velocity dispersion (averaged over a time range of about 100 Myr) are means over the whole set of the 10 N-body simulations performed for each model. A summary of the results is given in Tables 3–5 for sample2, sample1, and sample0, respectively. In Table 6, we summarize the properties of the clusters (number of stars, mass, and percentage of binaries) averaged for each model at 1.5 Gyr for the three samples.

Since binaries are usually more luminous (and also more massive, so less likely to escape) than single stars their contribution to the sample results larger than the contribution of individual stars. Such an effect is thus reflected in the percentage of binary at that time.

Considering sample2, from Figure 3 (first column, top panel) and Table 3, we note the expected result that the velocity dispersion estimated with method 1 ($\sigma_{\rm tot}$) is significantly larger, being in the range between $1.215\ {\rm km\,s^{-1}} \leqslant \sigma_{\rm tot} \leqslant 4.715\ {\rm km\,s^{-1}}$, with respect to the velocity dispersion derived with the other methods. Actually, in this case, the binary orbital motion inflates the estimate of the velocity dispersion with respect to the global orbital motion. On the other hand, when evaluating the velocity dispersion with method 3, thus weighing the binary contribution with the luminosity of the components, the result ranges between $0.445 \leqslant \sigma_{\rm lum}\ ({\rm km\,s^{-1}}) \leqslant 1.405$. Both $\sigma_{\rm tot}$ and $\sigma_{\rm lum}$ increase as the fraction of binaries in the sample increases.

On the contrary, the velocity dispersion derived with method 2 ($\sigma_{\rm cm}$) is independent of the binary content in the sample as shown in Figure 3. In fact, it does not show any trend and correlation with the fraction of binaries in the sample. The velocity dispersion obtained with such a method is much smaller, ranging between $0.2\ {\rm km\,s^{-1}} \leqslant \sigma_{\rm cm} \leqslant 0.3\ {\rm km\,s^{-1}}$, than when considering all stars individually.

We also estimated the velocity dispersion excluding binary stars (method 4): the velocity dispersion estimated in this way, $\sigma_{\rm sing}$, is very similar to $\sigma_{\rm cm}$ for all the samples.

Similar results are found for sample1 (Figure 3, second column and Table 4) and for sample0 (Figure 3, third column and Table 5). As the luminosity threshold increases (from sample2 to sample0) the velocity dispersion estimated with $\sigma_{\rm tot}$ and $\sigma_{\rm lum}$ increases too. This outcome is coherent with the fact that such methods are binary-dependent (the more luminous the sample, the larger the fraction of binaries).

If we compare the models studied, see top and bottom rows of Figure 3, we notice that the "virial" models A, B, and C show generally smaller values of the velocity dispersion with respect to subvirial models D, E, and F. Such an outcome is common to all the three samples and it is evident for $\sigma_{\rm tot}$ and $\sigma_{\rm lum}$. This effect is a combined consequence of the different

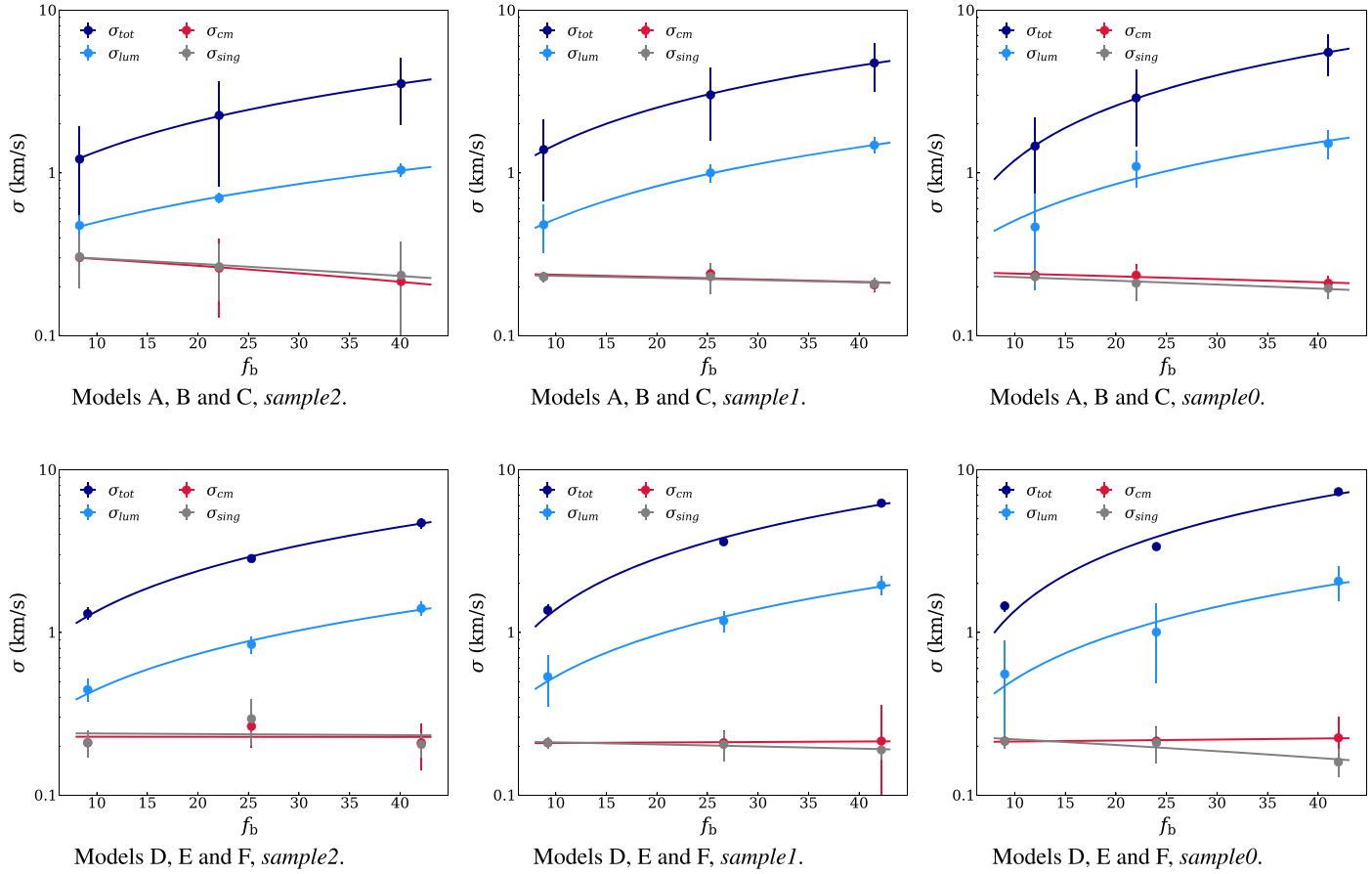

Models A, B and C, *sample2*. Models A, B and C, *sample1*. Models A, B and C, *sample0*.

Models D, E and F, *sample2*. Models D, E and F, *sample1*. Models D, E and F, *sample0*.

Figure 3. Velocity dispersions estimated according to the four methods described in Section 2 vs. the percentage of binaries at 1.5 Gyr ±50 Myr (see Table 6) for models A, B, and C (top panels), and D, E, and F (bottom panels) for sample2, sample1, and sample0, respectively, from left to right.

Table 3
The Velocity Dispersions (in Kilometers Per Second) Obtained with Each Method Described in Section 2.2, for Sample2

Sample2				
Model	$\sigma_{\rm tot}$	$\sigma_{\rm cm}$	$\sigma_{\rm lum}$	$\sigma_{\rm sing}$
A	1.215 ± 0.109	0.302 ± 0.063	0.475 ± 0.075	0.305 ± 0.069
B	2.255 ± 0.106	0.260 ± 0.032	0.700 ± 0.052	0.265 ± 0.041
C	3.530 ± 0.341	0.215 ± 0.063	1.040 ± 0.096	0.235 ± 0.141
D	1.305 ± 0.117	0.210 ± 0.036	0.445 ± 0.073	0.210 ± 0.039
E	2.845 ± 0.266	0.265 ± 0.069	0.845 ± 0.101	0.295 ± 0.093
F	4.715 ± 0.523	0.210 ± 0.066	1.405 ± 0.142	0.205 ± 0.034

Note. The columns indicate, from left to right (1) the model ID, (2) the velocity dispersion obtained with method 1 ($\sigma_{\rm tot}$), (3) the velocity dispersion obtained with method 2 ($\sigma_{\rm cm}$), (4) the velocity dispersion obtained with method 3 ($\sigma_{\rm lum}$), (5) the velocity dispersion obtained with method 4 ($\sigma_{\rm sing}$). The error of the velocity dispersion is evaluated according to its standard deviation measures.

fraction of binary stars between models on an initial virial and subvirial equilibrium as described in Table 6. On the other hand, the velocity dispersion $\sigma_{\rm cm}$ and that obtained from single stars, $\sigma_{\rm sing}$, match each other very well, over the three samples.

3.3. Time Evolution of the Velocity Dispersion

In Figure 4 we show the evolution of the velocity dispersion averaged over all the simulations of each of the six models studied (A, B, and C: top panels, left to right; C, D, and E: bottom panels, left to right) for sample2. We indicate with different line-style the velocity dispersion estimated with the four methods explained in Section 2.2.

As expected, $\sigma_{\rm tot}$ is at any time larger than the velocity dispersion estimated with the other methods.

For the sake of clarity Figure 5 displays a comparison among $\sigma_{\rm sing}$, $\sigma_{\rm lum}$, and $\sigma_{\rm cm}$ for models B (left panel) and E (right panel) that shows the overlap between $\sigma_{\rm cm}$ and $\sigma_{\rm sing}$. This outcome is

Table 4
Same as Table 3 but for Sample1

Sample1				
Model	$\sigma_{\rm tot}$	$\sigma_{\rm cm}$	$\sigma_{\rm lum}$	$\sigma_{\rm sing}$
A	1.390 ± 0.227	0.230 ± 0.013	0.480 ± 0.158	0.230 ± 0.016
B	3.015 ± 0.424	0.240 ± 0.034	1.000 ± 0.124	0.230 ± 0.049
C	4.735 ± 0.585	0.205 ± 0.020	1.480 ± 0.170	0.208 ± 0.019
D	1.370 ± 0.303	0.210 ± 0.012	0.535 ± 0.185	0.210 ± 0.016
E	3.610 ± 0.741	0.210 ± 0.040	1.180 ± 0.173	0.205 ± 0.042
F	6.235 ± 1.003	0.215 ± 0.145	1.955 ± 0.260	0.190 ± 0.024

Table 5
Same as Table 3 but for Sample0

Sample0				
Model	$\sigma_{\rm tot}$	$\sigma_{\rm cm}$	$\sigma_{\rm lum}$	$\sigma_{\rm sing}$
A	1.460 ± 0.561	0.235 ± 0.021	0.465 ± 0.275	0.230 ± 0.025
B	2.888 ± 0.558	0.235 ± 0.039	1.095 ± 0.277	0.210 ± 0.047
C	5.505 ± 1.082	0.210 ± 0.023	1.515 ± 0.300	0.195 ± 0.027
D	1.455 ± 0.724	0.215 ± 0.015	0.555 ± 0.331	0.215 ± 0.022
E	3.370 ± 1.427	0.215 ± 0.048	1.005 ± 0.513	0.210 ± 0.052
F	7.325 ± 1.561	0.225 ± 0.079	2.065 ± 0.502	0.160 ± 0.031

Table 6
Parameters Characterizing the Cluster Stellar Population for the Three Samples Studied, at $t = 1.5$ Gyr

	Sample2			Sample1			Sample0		
Model	$\langle N \rangle$	$\langle M_{\rm cl} \rangle$ $(M_\odot)$	$\langle f_b \rangle$ (%)	$\langle N \rangle$	$\langle M_{\rm cl} \rangle$ $(M_\odot)$	$\langle f_b \rangle$ (%)	$\langle N \rangle$	$\langle M_{\rm cl} \rangle$ $(M_\odot)$	$\langle f_b \rangle$ (%)
A	392	277	8.3	136	156	8.8	50	81	12.0
B	441	266	22.1	138	137	25.3	54	73	22.3
C	507	278	40.1	168	147	41.5	68	74	41.0
D	352	251	9.1	109	134	9.2	47	75	9.0
E	377	251	25.3	124	135	26.6	50	66	24.1
F	444	275	42.1	155	141	42.2	67	81	42.1

Note. The columns represent (from left to right): (1) the model ID, (2) the total number of stars (N), (3) the mass of the cluster ($M_{\rm cl}$), and (4) the percentage of binary stars (f_b). The reported values are averaged over all the simulations performed for each model.

typical of any model as anticipated by the results of Section 3.2. Cluster models on an initial virial equilibrium (A, B, and C) show lower values (a factor of two) of σ with respect to initially subvirial models (D, E, and F).

We notice a general decreasing of the velocity dispersion with time, independently on the method, that is common to all the models studied. The velocity dispersion decreases as a consequence of the evolution of the clusters that, as discussed in Section 3.1, undergo mass loss due to stellar evolution and dynamics in the form of escaping stars.

3.4. Dynamical Mass Estimates

The simplest way to estimate the mass of a star cluster is by mean of the assumption of virial equilibrium, $Q = 1$. In this case the dynamical (or virial) mass M_d of a star cluster can be estimated with the following relation (Spitzer 1987):

$$M_d = \frac{\eta\, \sigma_{\rm 1D}^2\, R_{\rm eff}}{G}, \tag{6}$$

where $\sigma_{\rm 1D}$ is the (1D, i.e., along the line of sight) velocity dispersion, G is the gravitational constant, $R_{\rm eff}$ is the effective

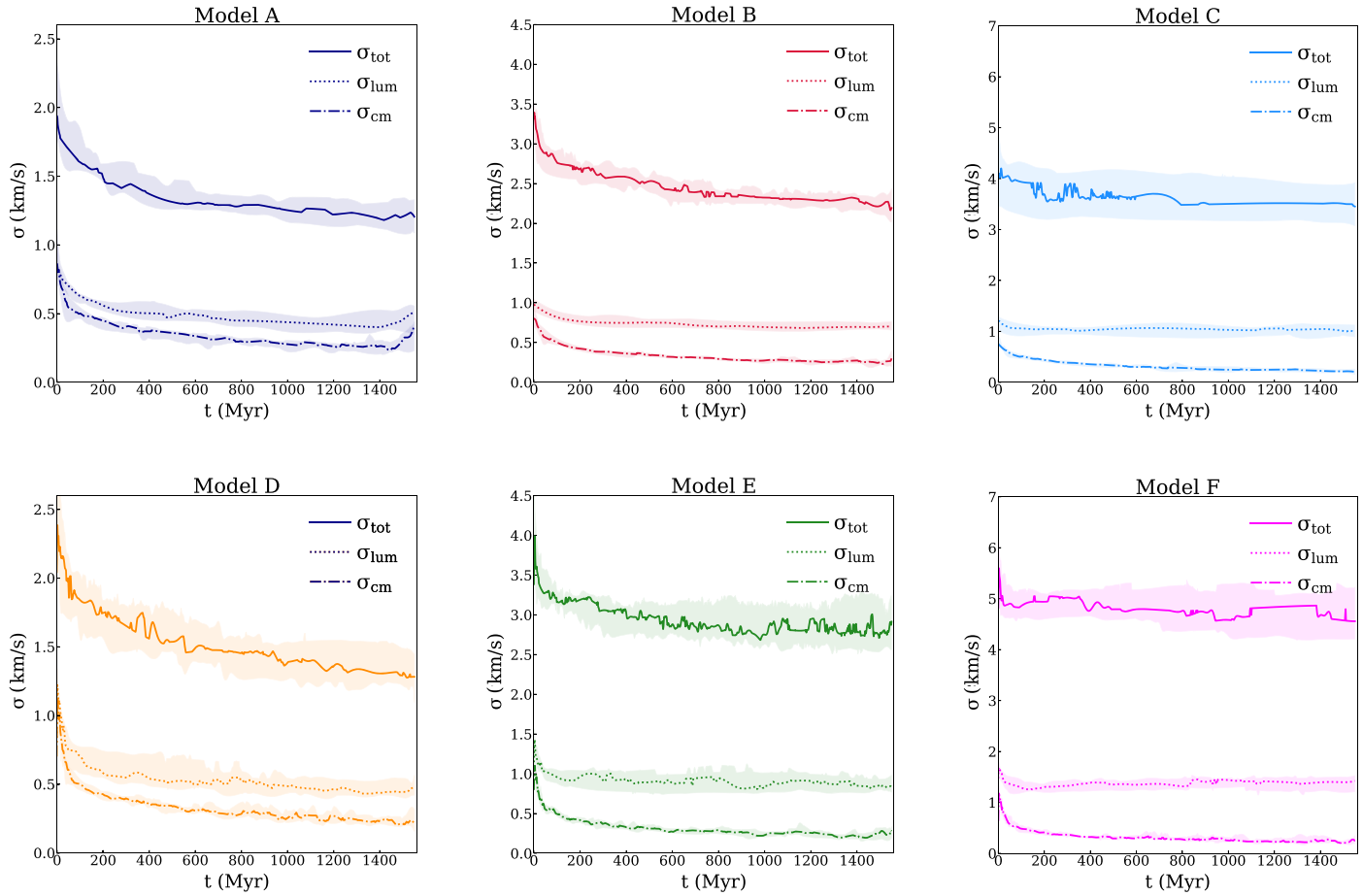

Figure 4. Time evolution of the various velocity dispersions for each model of sample2. The different lines represent the different method used to estimate σ: $\sigma_{\rm tot}$ solid line, $\sigma_{\rm lum}$ dotted line and $\sigma_{\rm cm}$ dotted–dashed line. The shaded region on each line indicates the error which is estimate as the standard deviation of the measures of σ. For display clarity, the results of $\sigma_{\rm sing}$ are not plotted here (see Figure 5).

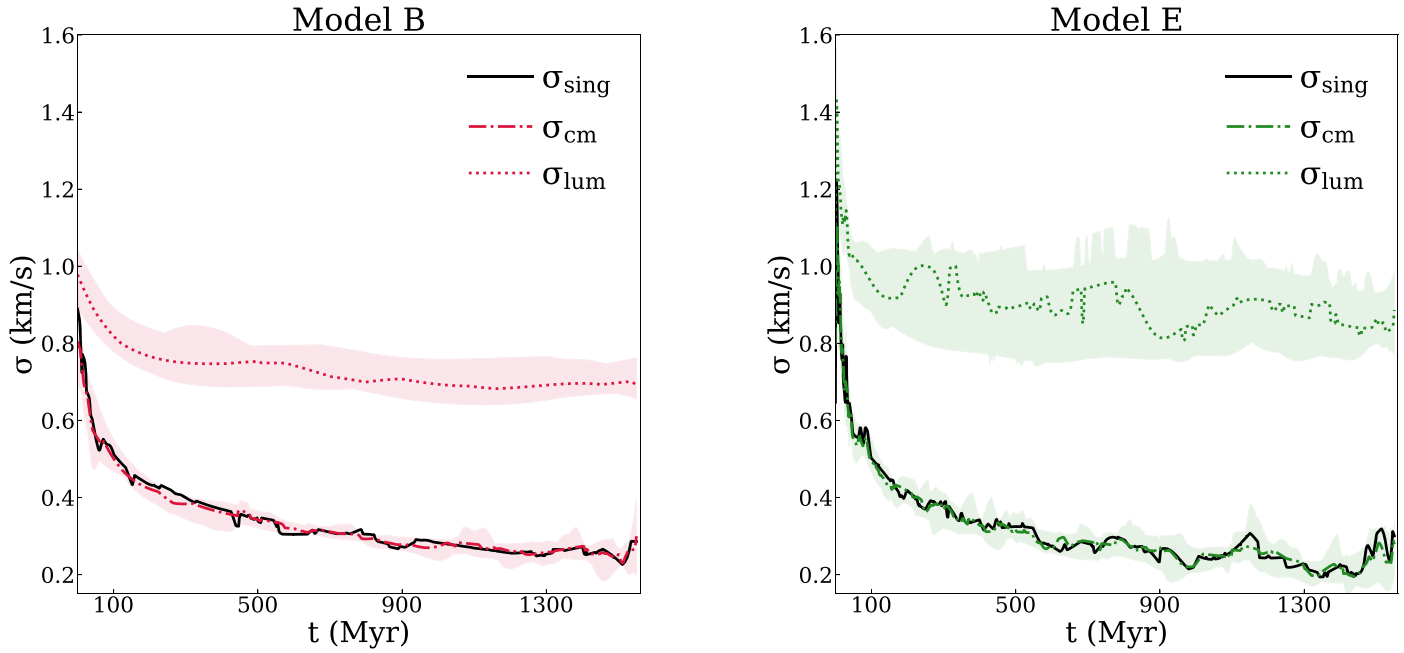

Figure 5. Enlargement of Figure 4 for models B and E showing the evolution of $\sigma_{\rm sing}$ (black line), $\sigma_{\rm cm}$ (dotted–dashed line), and $\sigma_{\rm lum}$ (dotted line). The behaviors of $\sigma_{\rm cm}$ and $\sigma_{\rm sing}$ overlap each other in both the models.

Table 7
Ratios of Various Determinations of σ^2 with Respect to $\sigma^2_{\rm cm}$, which Would Be the Correct One to Provide the Cluster Dynamical Mass, in Sample2, Sample1, and Sample0

	Sample2			Sample1			Sample0		
Model	$\sigma^2_{\rm tot}/\sigma^2_{\rm cm}$	$\sigma^2_{\rm lum}/\sigma^2_{\rm cm}$	$\sigma^2_{\rm sing}/\sigma^2_{\rm cm}$	$\sigma^2_{\rm tot}/\sigma^2_{\rm cm}$	$\sigma^2_{\rm lum}/\sigma^2_{\rm cm}$	$\sigma^2_{\rm sing}/\sigma^2_{\rm cm}$	$\sigma^2_{\rm tot}/\sigma^2_{\rm cm}$	$\sigma^2_{\rm lum}/\sigma^2_{\rm cm}$	$\sigma^2_{\rm sing}/\sigma^2_{\rm cm}$
A	16.2	2.5	1.020	36.5	4.4	1.00	38.6	3.9	0.9
B	75.2	7.3	1.039	157.8	17.4	0.918	151.1	21.7	0.8
C	269.6	23.4	1.195	533.5	52.1	1.029	687.2	52.1	0.8
D	38.6	4.5	1.000	42.5	6.5	1.000	45.7	6.6	1.0
E	115.2	10.2	1.239	295.4	31.6	0.953	245.3	21.8	0.9
F	504.1	44.7	0.953	841.0	82.7	0.781	1060.8	84.2	0.5

Table 8
Values of the Parameters in the Log-Linear Fitting Formula Equation (7) of the Results of Table 7 for Each Sample and Each Model

	Sample2				Sample1				Sample0			
	Model A, B, C		Model D, E, F		Model A, B, C		Model D, E, F		Model A, B, C		Model D, E, F	
	a	b	a	b	a	b	a	b	a	b	a	b
$\sigma^2_{\rm tot}/\sigma^2_{\rm cm}$	1.71	−0.95	1.52	0.18	1.8	−0.53	1.8	−0.3	2.34	−2.18	2.17	−1.22
$\sigma^2_{\rm lum}/\sigma^2_{\rm cm}$	1.51	−2.51	1.53	−2.18	2	−3.5	1.9	−2.9	1.68	−2.29	1.83	−2.48
$\sigma^2_{\rm sing}/\sigma^2_{\rm cm}$	0.03	−0.06	−0.02	0.07	0.05	−0.17	0.01	−0.04	−0.03	−0.04	−0.38	0.9

radius of the cluster, usually assumed as the half light radius of the systems (Gieles et al. 2010), and η is a dimensionless factor that depends on the cluster density profile (in the ideal case of a self-gravitating homogeneous sphere of radius $R_{\rm eff}$ in energy equipartition, $\eta = 5$).

It is relevant to note that the assumption of virial equilibrium is questionable for open-star clusters in our Galaxy because of the tidal galactic field, which can be relevant to the sizes of these star clusters (through differential rotational velocity).

Actually, what likely affects the dynamical mass estimate is the presence of binary stars in the stellar system, because they would naturally induce a bias of σ due to the fact that their pair orbits may increase the value of σ significantly. Once inserted in Equation (6), this leads to an overestimate even if the assumption of global virial equilibrium is valid.

Using our simulations of isolated open clusters containing an evolving binary population we can make a straightforward comparison between the different dynamical mass estimates derived by each of the methods described before. The comparison is done by measuring the various ratios between the σ^2 derived with each method and the $\sigma^2_{\rm cm}$ which, in its turn, would be the one giving the correct evaluation of mass.

The results of this analysis are summarized in Table 7 for the three luminosity-limited samples.

The overestimate of the dynamical mass produced by method 1 is large in all our models and samples. We find $16.2 < \sigma^2_{\rm tot}/\sigma^2_{\rm cm} < 504.1$ for sample2, $36.5 < \sigma^2_{\rm tot}/\sigma^2_{\rm cm} < 841$ for sample1, and $38.6 < \sigma^2_{\rm tot}/\sigma^2_{\rm cm} < 1060.8$ for sample0. As expected, the overestimate increases with the fraction of binaries. Moreover, the bias is greater for the subvirial models D, E, and F. This difference reflects their larger fraction of binaries as estimated at 1.5 Gyr (see Table 6). Since models on an initial subvirial state show a high percentage of binaries, their velocity dispersion $\sigma_{\rm tot}$ is larger yielding to a significant overestimate of M_d with respect to models with a lower fraction of binaries.

A similar outcome is found when considering $\sigma^2_{\rm lum}$. The overestimate of the mass reflects the corresponding velocity dispersion variation, $2.5 < \sigma^2_{\rm lum}/\sigma^2_{\rm cm} < 44.7$ for sample2, $4.4 < \sigma^2_{\rm lum}/\sigma^2_{\rm cm} < 82.7$ for sample1, and $3.9 < \sigma^2_{\rm lum}/\sigma^2_{\rm cm} < 84.2$ for sample0. As already mentioned, method 3 is the method that better mimics what observations give for measurements of the velocity dispersion of a star cluster. Thus, the results reported in column 2 of each box of Table 7 provide a reliable estimate of the correction to apply to observations to account for the binary population of the stellar system.

On the other side when we estimate the ratio $\sigma^2_{\rm sing}/\sigma^2_{\rm cm}$ we obtain values very close to 1. This outcome reflects what we derived in Section 3.2.

In Table 8 we report, for each sample, the parameters of log-linear fits of the results of Table 7:

$$\log(\sigma_i/\sigma_{\rm cm})^2 = a_i \log f_b + b_i, \tag{7}$$

where σ_i for $i = 1$, 2, and 3 corresponds, respectively, to $\sigma_{\rm tot}$, $\sigma_{\rm lum}$, and $\sigma_{\rm sing}$.

Now, recalling Equation (6), we can see that the value of the dynamical mass as estimated by observations is actually

$$\log \frac{M_{d,\rm obs}}{M_d} = \log\left(\frac{\sigma_i}{\sigma_{\rm cm}}\right)^2, \tag{8}$$

where $\log(\sigma_i/\sigma_{\rm cm})^2$ come from Equation (7). The formula above is a good correction formula to use to have a proper estimate of the virial mass from observed values of velocity dispersion biased by the presence of a binary population.

Given the values in Table 7, taking as the most representative sample that with the deepest luminosity (sample2) and calling the most likely σ determination $\sigma_{\rm lum}$, we determine that the logarithmic ratio between the observational and correct dynamical mass estimate varies in the range $0.4 \leqslant M_{d,\rm obs}/M_d \leqslant 1.4$ for $0.08 \leqslant f_b \leqslant 0.40$ in the virial models (A, B, C) and in the range $0.7 \leqslant M_{d,\rm obs}/M_d \leqslant 1.7$ for

$0.09 \leqslant f_b \leqslant 0.42$ in the subvirial models (D, E, F). This indicates an overestimate from a factor of 2.5 to a factor of 45, which is absolutely nonnegligible.

4. Summary and Conclusions

In this work we have presented a large suite of numerical simulations performed with the high precision, direct summation, NBODY7 code with the aim to investigate the effect of the presence of binary stars in the determination of the dynamical mass of stellar systems.

In particular, we focused our attention on models of Galactic open clusters, since these systems harbor abundant populations of binary stars, and are made of a relatively small number of stars, which makes numerical simulations affordable in terms of computational effort and, hence, allows an easier exploration of the parameter space.

In this study, we considered clusters containing, initially, 1000 stars, spanning a wide range of initial conditions, including different primordial binary fractions (5%, 15%, and 30%) and initial virial ratios ($Q_0 = 2K_0/|W_0|$) $Q_0 = 0.5$ and $Q_0 = 1$. We followed the evolution of each model up to 1.5 Gyr. Our simulations neglected the effect of the tidal field of the Milky Way, which we plan to include in the future.

The time evolution of various models' mass and half-mass radius were as expected: the mass decreases in all models, while the half-mass radius increases because of the combined effects of stellar evolution and two/three-body encounters that produce escapers. As expected, in subvirial ($Q_0 = 0.5$) models the mass loss is more significant than in initially virialized ($Q_0 = 1$) systems.

In addition, for each model we looked at the internal velocity dispersion. In detail, we normalized each estimate of the velocity dispersion ($\sigma_{\rm sing}$, $\sigma_{\rm tot}$, and $\sigma_{\rm lum}$) to $\sigma_{\rm cm}$, this latter being the one that best represents the actual kinetic content of the cluster, so it would be the proper one to evaluate a virial mass. The various estimates of the velocity dispersion we used have the aim to reproduce what observers obtain as estimates of the velocity dispersion of a star cluster.

Independently of the adopted initial model and of the specific velocity dispersion estimate considered, a clear trend emerges of larger velocity dispersion at larger binary fractions. This, in turn, produces an overestimate of the cluster dynamical mass when computed using blindly Equation (6). The overestimate depends on the way the velocity dispersion is derived. For reasonable values of the actual binary percentage (8%–42%) it can be up to a factor of 45. This implies that neglecting in part or completely the binary population in a cluster has a profound impact in the total mass estimate.

To take the binary effect into account, we provide in Section 3.4 fitting formulae which can be used to correct the cluster mass evaluation whenever some estimate of the binary fraction is available.

This has an impact on Galactic open clusters that is limited by the increasing precision of observational data which, nowadays, makes it possible to infer the binary fraction and the mass with enough precision from photometry only (Seleznev et al. 2017; Borodina et al. 2019). However, when considering other stellar systems, like dwarf galaxies in the Local Group, it is clear that a quantitative insight of the overestimate of the velocity dispersion caused by the binary population together with the assumption of virialization could be extremely helpful to determine the quantity of dark matter present. We are aware that the application of the present results to dwarf spheroidal galaxies can be done just in a tentative way, because the primordial binary fraction and their evolution due to the internal dynamics are, likely, significantly different from those in open clusters.

ORCID iDs

Sara Rastello https://orcid.org/0000-0002-5699-5516
Giovanni Carraro https://orcid.org/0000-0002-0155-9434
Roberto Capuzzo-Dolcetta https://orcid.org/0000-0002-6871-9519

References

Aarseth, S. J., & Lecar, M. 1975, ARA&A, 13, 1
Apai, D., Bik, A., Kaper, L., Henning, T., & Zinnecker, H. 2007, ApJ, 655, 484
Arca-Sedda, M., Capuzzo-Dolcetta, R., Antonini, F., & Seth, A. 2015, ApJ, 806, 220
Binney, J., & Tremaine, S. 2008, Galactic Dynamics (2nd ed.; Princeton, NJ: Princeton Univ. Press)
Borodina, O. I., Seleznev, A. F., Carraro, G., & Danilov, V. M. 2019, ApJ, 874, 127
Carraro, G., Baume, G., Seleznev, A. F., & Costa, E. 2017, Ap&SS, 362, 128
Chen, L., de Grijs, R., & Zhao, J. L. 2007, AJ, 134, 1368
de la Fuente Marcos, R., & de la Fuente Marcos, C. 2008, ApJ, 672, 342
Fan, X., Burstein, D., Chen, J.-S., et al. 1996, AJ, 112, 628
Fleck, J.-J., Boily, C. M., Lançon, A., & Deiters, S. 2006, MNRAS, 369, 1392
Geha, M., Willman, B., Simon, J. D., et al. 2009, ApJ, 692, 1464
Geller, A. M., & Mathieu, R. D. 2012, AJ, 144, 54
Gieles, M., Sana, H., & Portegies Zwart, S. F. 2010, MNRAS, 402, 1750
Goodman, J., & Hut, P. 1989, Natur, 339, 40
Goodwin, S. P. 2010, RSPTA, 368, 851
Goodwin, S. P., & Kroupa, P. 2005, A&A, 439, 565
Heggie, D., & Hut, P. 2003, The Gravitational Million-Body Problem: A Multidisciplinary Approach to Star Cluster Dynamics (Cambridge: Cambridge Univ. Press)
Heggie, D. C. 1975, MNRAS, 173, 729
Hut, P., McMillan, S., Goodman, J., et al. 1992, PASP, 104, 981
Jeans, J. H. 1919, MNRAS, 79, 408
Ji, J., & Bregman, J. N. 2013, ApJ, 768, 158
Ji, J., & Bregman, J. N. 2015a, arXiv:1505.00016
Ji, J., & Bregman, J. N. 2015b, ApJ, 807, 32
Kharchenko, N. V., Piskunov, A. E., Schilbach, E., Röser, S., & Scholz, R. D. 2013, A&A, 558, A53
Koposov, S. E., Gilmore, G., Walker, M. G., et al. 2011, ApJ, 736, 146
Kouwenhoven, M. B. N., Brown, A. G. A., Goodwin, S. P., Portegies Zwart, S. F., & Kaper, L. 2008, AN, 329, 984
Kouwenhoven, M. B. N., Brown, A. G. A., Portegies Zwart, S. F., & Kaper, L. 2007, A&A, 474, 77
Kouwenhoven, M. B. N., & de Grijs, R. 2008, A&A, 480, 103
Kroupa, P. 1995, MNRAS, 277, 1491
Kroupa, P. 2001, MNRAS, 322, 231
Kustaanheimo, P., & Stiefel, E. 1965, JRAM, 218, 204
Martinez, G. D., Minor, Q. E., Bullock, J., et al. 2011, ApJ, 738, 55
Mathieu, R. D. 1994, ARA&A, 32, 465
McConnachie, A. W. 2012, AJ, 144, 4
McMillan, S., & Hut, P. 1994, ApJ, 427, 793
McMillan, S., Hut, P., & Makino, J. 1990, ApJ, 362, 522
McMillan, S., Hut, P., & Makino, J. 1991, ApJ, 372, 111
Mikkola, S., & Aarseth, S. J. 1998, NewA, 3, 309
Mikkola, S., & Tanikawa, K. 1999, MNRAS, 310, 745
Moll, S. L., de Grijs, R., Mengel, S., Smith, L. J., & Crowther, P. A. 2009, Ap&SS, 324, 177
Muñoz, R. R., Carlin, J. L., Frinchaboy, P. M., et al. 2006, ApJL, 650, L51
Nitadori, K., & Aarseth, S. J. 2012, MNRAS, 424, 545
Plummer, H. C. 1911, MNRAS, 71, 460
Portegies Zwart, S. F., McMillan, S. L. W., Hut, P., & Makino, J. 2001, MNRAS, 321, 199
Portegies Zwart, S. F., & Yungelson, L. R. 1998, A&A, 332, 173
Sana, H., de Koter, A., de Mink, S. E., et al. 2013, A&A, 550, A107

Sana, H., Gosset, E., & Evans, C. J. 2009, MNRAS, 400, 1479
Sana, H., Gosset, E., Nazé, Y., Rauw, G., & Linder, N. 2008, MNRAS, 386, 447
Sana, H., James, G., & Gosset, E. 2011, MNRAS, 416, 817
Seleznev, A. F., Carraro, G., Capuzzo-Dolcetta, R., Monaco, L., & Baume, G. 2017, MNRAS, 467, 2517
Simon, J. D., Geha, M., Minor, Q. E., et al. 2011, ApJ, 733, 46
Spencer, M. E., Mateo, M., Olszewski, E. W., et al. 2018, AJ, 156, 257
Spencer, M. E., Mateo, M., Walker, M. G., et al. 2017, AJ, 153, 254
Spitzer, L. 1987, Dynamical Evolution of Globular Clusters (Princeton, NJ: Princeton Univ. Press)
Terlevich, E. 1987, MNRAS, 224, 193
Tofflemire, B. M., Gosnell, N. M., Mathieu, R. D., & Platais, I. 2014, AJ, 148, 61
Trenti, M., Ardi, E., Mineshige, S., & Hut, P. 2007, MNRAS, 374, 857
Vesperini, E. 2010, RSPTA, 368, 829